

Various Coordination Modes of the Bis(di(*o*-*N,N*-dimethylaniliny)phosphino)methane Ligand in Mononuclear and Binuclear Complexes of Group 8 and Group 9 Metals

James N. L. Dennett,[†] Matthias Bierenstiel,[†] Michael J. Ferguson,[‡] Robert McDonald,[‡] and Martin Cowie^{*†}

Department of Chemistry, University of Alberta, Edmonton, Alberta, T6G 2G2, Canada, and X-ray Crystallography Laboratory, University of Alberta, Edmonton, Alberta, T6G 2G2, Canada

Received September 22, 2005

The synthesis and characterization of a series of compounds involving the bis(di(*o*-*N,N*-dimethylaniliny)phosphino)methane (dmamp) ligand are described. The mononuclear complexes [MCl(CO)(*P,N*-dmamp)] (M = Rh, Ir) have a square-planar geometry in which the dmamp ligand chelates via a phosphine functionality and an adjacent amino group. The carbonyl ligand lies opposite the amine, while the chloro ligand is trans to the phosphine. The related complex [RhI(CO)(*P,N*-dmamp)] has also been prepared. All compounds are highly fluxional by at least three independent processes, as discussed for the rhodium–chloro species. A diiridium complex, [Ir₂Cl₂(CO)₂(*P,N,P',N'*-dmamp)], and the closely related rhodium/iridium analogue, [RhIrCl₂(CO)₂(*P,N,P',N'*-dmamp)], have been prepared in which the metals are bridged by the diphosphine group while an amino group at each end of the diphosphine is also coordinating to each metal on opposite faces of the M₂P₂ plane (M = Ir or Rh). For the Ir₂ species, the carbonyl and chloro groups are again shown to be opposite the amine and phosphine functionalities, respectively. The mononuclear complex [Ru(CO)₃(*P,P'*-dmamp)] has also been prepared. In contrast to the mononuclear species of rhodium and iridium, the dmamp group chelates the ruthenium center through both phosphorus atoms, occupying one axial and one equatorial site of Ru in a distorted trigonal bipyramidal geometry. Reaction of this Ru species with 1/2 equiv of the complexes [RhClL₂]₂ (L₂ = COD, (C₂H₄)₂, (CO)₂) yields the unstable Rh/Ru product [RhRuCl(CO)₃(*P,N,P',N'*-dmamp)].

Introduction

Studies of binuclear complexes, in which the adjacent metals can function in a synergic manner in their interactions with substrate molecules,¹ have been possible owing in a large part to the use of bridging ligands that hold the metals in close proximity even upon cleavage of metal–metal bonds. Arguably, the most frequently used family of bridging ligands are the diphosphines, of which bis(diphenylphosphino)methane (dppm) is the most common.² This ligand has been particularly prominent in chemistry involving late transition-metal complexes, to which it binds effectively. Not only does this ligand have a flexible bite that allows it to span a wide range in metal–metal separations, corresponding to a range in metal–metal bond orders, but the use of ³¹P

NMR spectroscopy has also been especially useful in characterization of its complexes.³

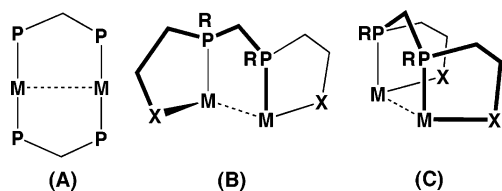
- (1) (a) Jones, N. D.; James, B. R. *Adv. Synth. Catal.* **2002**, *344*, 1. (b) Tsukada, N.; Ohba, Y.; Inoue, Y. *J. Organomet. Chem.* **2003**, *687*, 436. (c) Sola, E.; Bakhmutov, V. I.; Torres, F.; Elduque, A.; López, J. A.; Lahoz, F. J.; Werner, H.; Oro, L. A. *Organometallics* **1998**, *17*, 683. (d) Yuan, Y.; Jiménez, M. V.; Sola, E.; Lahoz, F. J.; Oro, L. A. *J. Am. Chem. Soc.* **2002**, *124*, 752. (e) Gauthier, S.; Scopelliti, R.; Severin, K. *Organometallics* **2004**, *23*, 3769. (f) Braunstein, P.; Clerc, G.; Morise, X. *Organometallics* **2001**, *20*, 5036. (g) Severin, K. *Chem. Eur. J.* **2002**, *8*, 1514. (h) Le Gendre, P.; Comte, V.; Michelot, A.; Moïse, C. *Inorg. Chim. Acta* **2003**, *350*, 289. (i) Wang, J.; Li, H.; Guo, N.; Li, L.; Stern, C. L.; Marks, T. J. *Organometallics* **2004**, *23*, 5112. (j) Man, M. L.; Zhou, Z. Y.; Ng, S. M.; Lau, C. P. *J. Chem. Soc., Dalton Trans.* **2003**, 3727. (k) Quebatte, L.; Scopelliti, R.; Severin, K. *Angew. Chem., Int. Ed.* **2004**, *43*, 1520. (l) Torkelson, J. R.; Antwi-Nsiah, F. H.; McDonald, R.; Cowie, M.; Prius, J. G.; Jalkanen, K. L.; DeKock, R. L. *J. Am. Chem. Soc.* **1999**, *121*, 3666. (m) Ristic-Petrovic, D.; Anderson, D. J.; Torkelson, J. R.; Ferguson, M. J.; McDonald, R.; Cowie, M. *Organometallics* **2005**, *24*, 3711.
- (2) See the following for examples: (a) Puddephatt, R. *J. Chem. Soc. Rev.* **1983**, *12*, 99. (b) Chaudret, B.; Delavaux, B.; Poilblanc, R. *Coord. Chem. Rev.* **1988**, *86*, 191.

* To whom correspondence should be addressed. E-mail: martin.cowie@ualberta.ca.

[†] Department of Chemistry.

[‡] X-ray Crystallography Laboratory.

Chart 1



Most of the late transition-metal complexes involving the dppm ligand have two such groups in a mutually trans arrangement at both metals as diagrammed in structure **A** in Chart 1 (ancillary ligands and dppm phenyl groups omitted; the dashed line indicates that a metal–metal bond may or may not be present). In such a geometry, access of substrates to the metals can be inhibited by the bulky dppm phenyl substituents, which project above and below the plane of the drawing. One approach to increasing accessibility to the metals is to substitute the phenyl groups with smaller alkyl groups.⁴ Another approach is to utilize diphosphines having pendent groups that can also chelate to the metals giving a cis arrangement at each metal as shown in structures **B** and **C**. In these geometries (but particularly for **C**) the cis chelates appear to allow better access to the metals at the sites opposite the donor groups. Two such bridging groups that have received recent attention are a series of tetraphosphines in which the pendent chelating groups are $\text{CH}_2\text{CH}_2\text{PR}_2$ ($\text{X} = \text{PR}_2$ in structure **B**), the chemistry of which has been pioneered by Stanley and co-workers⁵ and also studied by Süß-Fink,⁶ and the bis(di(*o*-*N,N*-dimethylaniliny)phosphino)methane (dmampm) ligand, in which the pendent groups, both chelated and dangling (R groups in structures **B** and **C**), are dimethylaniliny substituents ($\text{X} = \text{NMe}_2$, only ipso and ortho carbons of phenyl groups are shown for the chelated groups), recently reported by James and co-workers.^{7–9} We were intrigued by the possibility that dmampm could perform a dual role, in which the diphosphine moiety could bridge a pair of late transition metals, while the chelating amine groups might be labile, generating, in effect, linked pairs of hemilabile¹⁰ *P,N*-bound ligands at each metal. There has been significant recent interest in related hemilabile

groups involving phosphorus together with nitrogen,¹¹ and some of these systems have shown interesting catalytic activity.^{10d,e,12}

As noted above, our interest in dmampm is as a ligand that can bridge pairs of adjacent metals. Binuclear complexes in which the pairs of metals are either the same or different are currently of interest as potential catalysts,^{5,6,13} owing to the prospects of improved catalytic activity and/or selectivity as a result of the adjacent metals acting in a cooperative manner. In this regard, it has been proposed by Tsukada and co-workers¹⁴ that a cis-chelating ligand configuration at the adjacent metals, similar to those diagrammed in structures **B** and **C**, might be important in promoting the cooperative involvement of adjacent metals. In this paper we describe our attempts to generate mononuclear dmampm-containing precursors for use in synthesizing dmampm-bridged homo- and heterobinuclear complexes and outline our initial success in generating the targeted binuclear species.

Experimental Section

General Comments. All solvents were deoxygenated, dried (using appropriate drying reagents), distilled before use, and stored under nitrogen. The reactions were performed under an argon atmosphere using standard Schlenk techniques. $\text{RhCl}_3 \cdot 3\text{H}_2\text{O}$ and $\text{Ru}_3(\text{CO})_{12}$ were purchased from Strem Chemicals, and $[\text{NH}_4]_2[\text{IrCl}_6]$ was obtained from Vancouver Island Precious Metals. ¹³C-enriched CO (99.4% enrichment) was purchased from Isotec Inc. and Cambridge Isotope Laboratories (99% enrichment). The compounds $[\text{Rh}_2(\mu\text{-Cl})_2(\text{CO})_4]$,¹⁵ $[\text{Rh}_2(\mu\text{-Cl})_2(\text{COD})_2]$,¹⁶ $[\text{Rh}_2(\mu\text{-Cl})_2(\text{C}_2\text{H}_4)_4]$,¹⁷ and $[\text{Ir}_2(\mu\text{-Cl})_2(\text{COE})_4]$ ¹⁸ (COD = 1,5-cyclooctadiene; COE = cyclooctene) were prepared by the literature routes. The diphosphine ligand, bis(di(*o*-*N,N*-dimethylaniliny)phosphino)methane (dmampm), was prepared as previously reported.⁷

- (3) See the following for recent examples: (a) Trepanier, S. T.; Dennett, J. N. L.; Sterenberg, B. T.; McDonald, R.; Cowie, M. *J. Am. Chem. Soc.* **2004**, *126*, 8046. (b) Oldham, S. M.; Houllis, J. F.; Sleight, C. J.; Duckett, S. B.; Eisenberg, R. *Organometallics* **2000**, *19*, 2985. (c) Rashidi, M.; Kamali, K.; Jennings, M. C.; Puddephatt, R. J. *J. Organomet. Chem.* **2005**, *690*, 1600 and references therein.
- (4) (a) Jenkins, J. A.; Cowie, M. *Organometallics* **1992**, *11*, 2767. (b) Ara, I.; Fanwick, P. E.; Walton, R. A. *Inorg. Chem.* **1993**, *32*, 2958. (c) Kullberg, M. L.; Lemke, F. R.; Powell, D. R.; Kubiak, C. P. *Inorg. Chem.* **1985**, *24*, 3589. (d) Pamplin, C. B.; Rettig, S. J.; Patrick, B. O.; James, B. R. *Inorg. Chem.* **2003**, *42*, 4117. (e) Anderson, D. J.; Kramarz, K. W.; Eisenberg, R. *Inorg. Chem.* **1996**, *35*, 2688.
- (5) (a) Laneman, S. A.; Fronczek, F. R. and Stanley, G. G. *J. Am. Chem. Soc.* **1988**, *110*, 5585. (b) Broussard, M. E.; Juma, B.; Train, S. G.; Peng, W.-J.; Laneman, S. A.; Stanley, G. G. *Science* **1993**, *260*, 1784. (c) Matthews, R. C.; Howell, D. K.; Peng, W.-J.; Train, S. G.; Treleaven, W. D.; Stanley, G. G. *Angew. Chem., Int. Ed. Engl.* **1996**, *35*, 2253.
- (6) Süß-Fink, G. *Angew. Chem., Int. Ed. Engl.* **1994**, *33*, 67.
- (7) Jones, N. D.; Meessen, P.; Smith, M. B.; Losehand, U.; Rettig, S. J.; Patrick, B. O.; James, B. R. *Can. J. Chem.* **2002**, *80*, 1600.
- (8) Jones, N. D.; Foo, S. J. L.; Patrick, B. O.; James, B. R. *Inorg. Chem.* **2004**, *43*, 4056.
- (9) Foo, S. J. L.; Jones, N. D.; Patrick, B. O.; James, B. R. *Chem. Commun.* **2003**, 988.

- (10) (a) Jeffrey, J. C.; Rauchfuss, T. B. *Inorg. Chem.* **1979**, *18*, 2658. (b) Bader, A.; Lidner, E. *Coord. Chem. Rev.* **1991**, *108*, 27. (c) Slone, C. S.; Weinberger, D. A.; Mirkin, C. A. *Prog. Inorg. Chem.* **1999**, *48*, 233. (d) Espinet, P.; Soulantica, K. *Coord. Chem. Rev.* **1999**, *183–195*, 499. (e) Braunstein, P.; Naud, F. *Angew. Chem., Int. Ed.* **2001**, *40*, 680.
- (11) See the following for examples: (a) LeGall, I.; Laurent, P.; Soulier, E.; Salaün, J.-Y.; desAbbayes, H. *J. Organomet. Chem.* **1998**, *567*, 13. (b) Liu, X.; Eisenberg, A. H.; Stern, C. L.; Mirkin, C. A. *Inorg. Chem.* **2001**, *40*, 2940. (c) Romeo, R.; Scolaro, L. M.; Plutino, M. R.; Romeo, A.; Nicolo, F.; Del Zotto, A. *Eur. J. Inorg. Chem.* **2002**, 629. (d) Boubekeur, L.; Ricard, L.; Mézailles, N.; LeFoch, P. *Organometallics* **2005**, *24*, 1065. (e) Rankin, M. A.; McDonald, R.; Ferguson, M. J.; Stradiotto, M. *Organometallics* **2005**, *24*, 4981.
- (12) See the following for examples: (a) Helmchen, G.; Pfaltz, A. *Acc. Chem. Res.* **2000**, *33*, 336. (b) Ittel, S. D.; Johnson, L. K.; Brookhart, M. *Chem. Rev.* **2000**, *100*, 1169. (c) Alonso, M. A.; Casares, J. A.; Espinet, P.; Vallés, E.; Soulantica, K. *Tetrahedron Lett.* **2001**, *42*, 5697. (d) Sauthier, M.; Leca, F.; Toupet, L.; Réau, R. *Organometallics* **2002**, *21*, 1591. (e) Dahlenberg, L.; Götz, R. *Eur. J. Inorg. Chem.* **2004**, 888. (f) Parisel, S. L.; Adrio, L. A.; Pereiro, A. A.; Pérez, M. M.; Vila, J. M.; Hii, K. K. *Tetrahedron* **1998**, *54*, 12985. (g) Weng, Z.; Teo, S.; Koh, L. L.; Hor, T. S. A. *Angew. Chem., Int. Ed.* **2005**, *44*, 7560.
- (13) See the following for examples: (a) Steinhagen, H.; Helmchen, G. *Angew. Chem., Int. Ed. Engl.* **1996**, *35*, 2339. (b) Van den Beuken, E. K.; Feringa, B. L. *Tetrahedron* **1998**, *54*, 12985. (c) Ishii, Y.; Hidai, M. *Catal. Today* **2001**, *66*, 53. (d) Rowlands, G. J. *Tetrahedron* **2001**, *57*, 1865. (e) Rida, M. A.; Smith, A. K. *J. Mol. Catal. A: Chem.* **2003**, *202*, 87.
- (14) Tsukada, N.; Tamura, O.; Inoue, Y. *Organometallics* **2002**, *21*, 2521.
- (15) McCleverty, J. A.; Wilkinson, G. *Inorg. Synth.* **1966**, *8*, 211.
- (16) Giordano, G.; Crabtree, R. H. *Inorg. Synth.* **1979**, *19*, 218.
- (17) Cramer, R. *Inorg. Synth.* **1974**, *15*, 14.
- (18) Herde, J. L.; Lambert, J. C.; Senott, C. V. *Inorg. Synth.* **1974**, *15*, 18.

Table 1. Spectroscopic Data for the Compounds,

| IR (cm ⁻¹) ^a | NMR ^b δ (³¹ P{ ¹ H}) ^c | NMR ^b δ (¹ H) ^d | NMR ^b δ (¹³ C{ ¹ H}) ^d |
|-------------------------------------|--|---|---|
| | | [RhCl(CO)(<i>P,N</i> -dmapm) (1)] | |
| 1980 (s) | 40.9 (dd, ¹ J _{RhP} = 170 Hz, ² J _{PP} = 138 Hz), -41.8 (d, ² J _{PP} = 138 Hz) ^e | NMe ₂ : 3.29 (s, 3H), 2.99 (s, 3H), 2.79 (s, 6H), 2.65 (s, 3H), 2.26 (s, 6H), 1.54 (s, 3H) ^e CH ₂ : 3.15 (m, 1H) ^{e,f} NMe ₂ : 2.71 (s, 12H), 2.60 (s/br, 12H) ^g CH ₂ : 3.23 (s/br, 1H), 3.20 (s/br, 1H) ^g | NMe ₂ : 50.0 (m, 1C), 49.5 (s, 1C), 47.1 (s, 1C), 45.0 (br/m, 2C), 44.2 (m, 2C), 42.9 (s, 1C) ^e CH ₂ : 29.6 (m) ^e CO: 187.8 (dd, ¹ J _{RhC} = 73 Hz, ² J _{PC} = 19 Hz) ^e |
| | | [IrCl(CO)(<i>P,N</i> -dmapm) (2)] | |
| 1966 (s) | 14.2 (d, ² J _{PP} = 126 Hz), -41.8 (d, ² J _{PP} = 126 Hz) ^e | NMe ₂ : 3.28 (s, 3H), 3.00 (s, 3H), 2.71 (s, 6H), 2.55 (s, 3H), 2.23 (s, 6H), 1.54 (s, 3H) ^e CH ₂ : 3.45 (m, 2H) NMe ₂ : 3.30 (s/br, 3H), 3.14 (s/br, 3H), 2.73 (s/br, 6H), 2.22 (s/br, 6H), 2.53 (s/br, 6H) ^g CH ₂ : 3.39 (s/br, 2H) ^g | NMe ₂ : 50.4 (1C), 49.9 (1C), 47.3 (1C), 45.0 (2C), 44.1 (2C), 42.5 (1C) ^e CH ₂ : 29.3 (m) ^e CO: 172.0 (d, ² J _{PC} = 12 Hz) ^e |
| | | [RhI(CO)(<i>P,N</i> -dmapm) (3)] | |
| 1978 (s) | 37.1 (dd, ¹ J _{RhP} = 74 Hz, ² J _{PP} = 128 Hz), -41.3 (d, ² J _{PP} = 128 Hz) ^g | NMe ₂ : 2.78 (s/br, 12H), 2.60 (s, 12H) ^g CH ₂ : 3.23 (m, 2H) ^g | |
| | | [RhIrCl ₂ (CO) ₂ (<i>P,N,P',N'</i> -dmapm) (4)] | |
| 1989 (s), 1995 (sh) ^h | 41.6 (dd, ¹ J _{RhP} = 176 Hz, ² J _{PP} = 37 Hz, 1P), 13.9 (br, d, ² J _{PP} = 37 Hz) ^g | NMe ₂ : 3.81 (s, 3H), 3.65 (s, 3H), 2.96 (s, 3H), 2.91 (s, 3H), 2.71 (s, 6H), 2.34 (s, 3H), 2.31 (s, 3H) ⁱ CH ₂ : 4.85 (m, 1H), 4.78 (m, 1H) ⁱ | NMe ₂ : 52.5 (m, 1C), 51.6 (s, 1C), 47.6 (s, 2C), 47.4 (s, 2C), 45.2 (m, 1C), 43.6 (m, 1C) ^g CH ₂ : 25.8 (m) ^g CO: 187.8 (dd, ¹ J _{RhC} = 75 Hz, ² J _{PC} = 13 Hz), 171.0 (d, ² J _{PC} = 16 Hz) ^{g,j} |
| | | [Ir ₂ Cl ₂ (CO) ₂ (<i>P,N,P',N'</i> -dmapm) (5)] | |
| 1988 (s), 1979 (s/sh) | 13.9 (s, 2P) ^g | NMe ₂ : 3.73 (s, 6H), 2.89 (s, 6H), 2.68 (s, 6H), 2.55 (s, 6H) ^e CH ₂ : 5.08 (t, ² J _{HP} = 3.2 Hz, 2H) ^e NMe ₂ : 3.80 (s, 6H), 3.02 (s, 6H), 2.66 (br, 6H), 2.54 (br, 6H) ^g CH ₂ : 5.05 (t, ² J _{HP} = 13 Hz, 2H) ^g | NMe ₂ : 52.6 (2C), 50.9 (2C), 47.5 (2C), 47.15 (2C) ^e CH ₂ : 22.4 (t, ¹ J _{PC} = 17 Hz) ^e CO: 170.5 (d, ² J _{PC} = 8 Hz) ^e |
| | | [Ru(CO) ₃ (<i>P,P'</i> -dmapm) (6)] | |
| 1989 (s), 1910 (m), 1883 (m) | -21.0 (s, 2P) ^g | NMe ₂ : 2.12 (s, 24H) CH ₂ : 4.57 (t, ² J _{HP} = 9 Hz 2H) | NMe ₂ : 46.0 (s) ^e CH ₂ : 34.4 (m) ^e CO: 214.3 (t, ² J _{PC} = 15 Hz) ^e |
| | | RhRuCl(CO) ₃ (<i>P,N,P',N'</i> -dmapm) (7) | |
| 2001(s), 1908(m), 1726 (w) | 52.5 (dd, ¹ J _{RhP} = 77 Hz, ² J _{PP} = 102 Hz), 33.6 (d, ² J _{PP} = 102 Hz), ^e 50.5 (dd, ¹ J _{RhP} = 179 Hz, ² J _{PP} = 107 Hz), 34.2 (d, ² J _{PP} = 107 Hz) ^g | NMe ₂ : 3.74 (s, 3H), 3.03 (s, 3H), 2.76 (s, 6H), 2.55 (s, 3H), 2.54(s, 3H), 2.51 (s, 3H), 2.36 (s, 3H) ^e CH ₂ : 4.48 (m, 1H), 3.78 (m, 1H) ^e NMe ₂ : 3.73 (s, 3H), 3.08 (s, 3H), 2.77 (s, 6H), 61 (s/br, 6H), 2.49 (s, 6H) ^g CH ₂ : 4.56 (m, 2H) ^g | NMe ₂ : 61.6 (s, 1C), 55.5 (m, 1C), 50.7 (s, 1C), 50.1 (s, 1C), 47.6 (s, 1C), 46.7 (s, 1C), 44.1 (s, 2C) ^e CO: 250.1 (m), 202.9 (d, ² J _{PC} = 102 Hz), 197.2 (m), ^{e,k} 246.3 (m, ¹ J _{RhC} = 42 Hz, ² J _{P(Rh)C} = 1 Hz, ² J _{P(Ru)C} = 7 Hz), 203.1 (d, ² J _{PC} = 102 Hz), 197.3 (d, ² J _{PC} = 15 Hz) ^g |

^a IR abbreviations: s = strong, m = medium, w = weak, sh = shoulder. Dichloromethane solution; in units of cm⁻¹. ^b NMR abbreviations: s = singlet, d = doublet, t = triplet, m = multiplet, br = broad, dd = doublet of doublets. NMR data in CD₂Cl₂ unless otherwise indicated. ^c ³¹P chemical shifts referenced to external 85% H₃PO₄. ^d ¹H and ¹³C chemical shifts referenced to tetramethylsilane. Chemical shifts for the phenyl groups not given. ^e NMR data at -80 °C. ^f Signal of other CH₂ obscured by other peaks. ^g 27 °C. ^h Acetone. ⁱ NMR data at -40 °C. ^j ¹³C{¹H} NMR data obtained with ¹³CO enrichment. ^k The dmapm CH₂ not observed.

NMR spectra were recorded on either a Bruker AM-400 or a Varian Inova-400 spectrometer operating at 400.0 or 399.8 MHz, respectively, for ¹H, at 161.9 or 161.8 MHz, respectively, for ³¹P, and at 100.6 MHz for ¹³C nuclei (Bruker AM-400). Infrared spectra (KBr cell) were recorded on either a FTIR Bomem MB-100 spectrometer or a Nicolet Avator 370 DTGS spectrometer. Elemental analyses were performed by the Microanalytical Laboratory of this department. Electrospray ionization mass spectra were run on a Micromass Zabspec spectrometer in the department MS facility. In all cases, the distribution of isotope peaks for the appropriate parent ion matched very closely that calculated from the formulation given. Spectroscopic data for the compounds are given in Table 1.

Preparation of Compounds. (a) [RhCl(CO)(*P,N*-dmapm) (1).

A CH₂Cl₂ (20 mL) solution of [Rh₂(μ-Cl)₂(CO)₄] (133.0 mg; 0.341 mmol) was added dropwise to a CH₂Cl₂ solution of dmapm (401 mg; 0.721 mmol) at -78 °C over a 50 min period. The solution was allowed to warm slowly over 1 h and stirred for a further 3.5 h. The solvent was removed in vacuo to give a yellow residue. Dichloromethane (ca. 2 mL) was added, to give an orange solution which yielded a yellow precipitate of [RhCl(CO)(*P,N*-dmapm)] (1) (450 mg; 91.0%) upon the addition of *n*-pentane (60 mL). Crystals suitable for an X-ray crystallographic study were grown through layering a saturated CH₂Cl₂ solution of 1 with *n*-pentane. Anal. Calcd for C₃₄H₄₂ClN₄OP₂Rh: C, 56.50; H, 5.86; N, 7.75%.

Found: C, 56.14; H, 5.86; N, 7.46%. MS (EI): m/z 723.2 (M^+), 695.2 ($M^+ - CO$), 687.2 ($M^+ - Cl$), 659.2 ($M^+ - CO - Cl$).

(b) [IrCl(CO)(P,N-dmapm)] (2). Dichloromethane (10 mL) was added to a mixture of $[Ir_2(\mu-Cl)_2(COE)_4]$ (224 mg; 0.250 mmol) and dmapm (278 mg; 0.500 mmol). The solution was stirred for 5 min, purged with carbon monoxide for 5 min, and then was stirred under a CO atmosphere for a further 1 h. The solution was concentrated under vacuum to approximately 1 mL, and upon addition of *n*-pentane (30 mL) a yellow solid precipitated which was filtered yielding **(2)** (362 mg, 87%). Crystals suitable for an X-ray crystallographic study were grown by layering a saturated CH_2Cl_2 solution of **(2)** with *n*-pentane. Anal. Calcd for $C_{34}H_{42}ClN_4OP_2Ir$: C, 50.27; H, 5.21; N, 6.90%. Found: C, 50.66; H, 5.41; N, 6.51%. MS (EI): m/z 813.2 (M^+).

(c) [RhI(CO)(P,N-dmapm)] (3). Compound **(1)** (80.0 mg; 0.110 mmol) was dissolved in a mixture of methanol (30 mL) and dichloromethane (10 mL), to which solid KI (500 mg, 3.00 mmol) was added, and the reaction mixture was stirred at ambient temperature for 18 h. The solvent was completely removed under high vacuum, and the remaining solids were extracted with 10 mL of dichloromethane. The supernatant solution was carefully transferred to another flask via a cannula, and the solvent volume was reduced to approximately 1 mL. Addition of 20 mL of *n*-pentane produced a yellow-brown solid which was filtered and dried in vacuo, producing $[RhI(CO)(P,N-dmapm)]$ (**(3)**) (84.2 mg; 93.5%). Anal. Calcd for $C_{34}H_{42}IN_4OP_2Rh$: C, 50.14; H, 5.20; N, 6.88%. Found: C, 49.78; H, 5.35; N, 6.97%.

(d) [RhIrCl₂(CO)₂(P,N,P',N'-dmapm)] (4). Method i. To a solution of $[IrCl(CO)(P,N-dmapm)]$ (**(2)**) (249 mg; 0.306 mmol) dissolved in dichloromethane (10 mL) was added $[RhCl(COD)]_2$ (75.0 mg, 0.153 mmol). Carbon monoxide was passed through the reaction mixture for 10 min, and the solution was stirred at ambient temperature for 18 h. The resulting yellow solution was concentrated in vacuo to approximately 1 mL, and *n*-pentane (30 mL) was added, yielding a yellow solid which was filtered and dried in vacuo (269.8 mg; 90.0%).

Method ii. In an NMR tube, $[RhCl(CO)(P,N-dmapm)]$ (**(1)**) (8.0 mg; 0.011 mmol) and $[Ir_2(\mu-Cl)_2(COE)_4]$ (5.0 mg; 0.0055 mmol) were dissolved in 0.6 mL of CD_2Cl_2 . Carbon monoxide was passed through the solution at ambient temperature for 5 min, and an NMR spectrum was recorded after 1 h. The $^{31}P\{^1H\}$ spectrum of the resulting solution was identical to the product **(4)** obtained in method i. Yellow crystals were grown by layering a saturated CH_2Cl_2 solution of **(4)** with *n*-pentane. Anal. Calcd for $C_{35}H_{42}Cl_2IrN_4O_2P_2Rh$: C, 42.95; H, 4.33; N, 5.72%. Found: C, 42.88; H, 4.54; N, 5.71%.

(e) [Ir₂Cl₂(CO)₂(P,N,P',N'-dmapm)] (5). Method i. Dichloromethane (50 mL) was added to a mixture of $[Ir_2(\mu-Cl)_2(COE)_4]$ (309 mg; 0.340 mmol) and dmapm (200 mg; 0.360 mmol), and the orange solution was stirred for 15 min. Carbon monoxide was passed over the solution which was heated to reflux for 1.25 h, giving a dark red solution. (The reaction could also be carried out at ambient temperature but required a longer reaction time.) The heating was stopped, and carbon monoxide was passed through the solution for a further 2 h. The solution was then filtered through Celite, and the solvent was removed in vacuo, giving a red residue. Dichloromethane (ca. 2 mL) was added, followed by *n*-pentane (50 mL), giving $[Ir_2Cl_2(CO)_2(P,N,P',N'-dmapm)]$ (**(5)**) as an orange precipitate (250.0 mg; 67.8%).

Method ii. In an NMR tube, $[IrCl(CO)(P,N-dmapm)]$ (**(2)**) (20.0 mg; 0.0250 mmol) and $[Ir_2(\mu-Cl)_2(COE)_4]$ (11.0 mg; 0.0125 mmol) were dissolved in 0.6 mL of CD_2Cl_2 . Carbon monoxide was passed through the solution at ambient temperature for 5 min, and

the NMR spectrum was recorded after 1 h. The $^{31}P\{^1H\}$ spectrum was identical to the product described in method i, indicating quantitative conversion to compound **(5)**. Yellow/orange crystals suitable for an X-ray crystallographic study were grown by layering a saturated CH_2Cl_2 solution of **(5)** with *n*-pentane. Anal. Calcd for $C_{35}H_{42}Cl_2Ir_2N_4O_2P_2$: C, 39.39; H, 3.96; N, 5.25%. Found: C, 39.20; H, 3.96; N, 4.85%. MS (EI): m/z 1069.1 (M^+).

(f) [Ru(CO)₃(P,P'-dmapm)] (6). An *n*-pentane solution (140 mL) of $[Ru(CO)_4(\eta^2-C_2H_4)]$ was prepared photolytically with the use of $[Ru_3(CO)_{12}]$ (195.4 mg, 0.306 mmol) and an ethylene purge.¹⁹ The solution was then slowly added, in the dark, to a pentane (100 mL) suspension of dmapm (340.0 mg, 0.612 mmol), and the suspension was stirred overnight, giving an orange suspension. The solvent was removed in vacuo, and the orange residue was dissolved in Et_2O (70 mL) and filtered through Celite to remove any $[Ru_3(CO)_{12}]$. The solvent was removed, and pentane (20 mL) was added. The orange suspension was cooled to $-78^\circ C$, the solvent was removed by cannula, and the process was repeated, eventually giving (after drying) $[Ru(CO)_3(P,P'-dmapm)]$ (**(6)**) as a yellow/orange precipitate (340 mg, 75.1%). Yellow/orange crystals suitable for an X-ray crystallographic study were grown by the slow evaporation of a saturated CD_2Cl_2 solution. Anal. Calcd for $C_{36}H_{42}N_4O_3P_2Ru$: C, 58.29; H, 5.71; N, 7.55%. Found: C, 58.30; H, 5.65; N, 7.53%. MS (EI): m/z 742.2 (M^+).

(g) [RhRuCl(CO)₃(P,N,P',N'-dmapm)] (7). Method i. To a CD_2Cl_2 solution (0.3 mL) of $[Ru(CO)_3(P,P'-dmapm)]$ (**(6)**) (39.0 mg; 0.0526 mmol) was added slowly, over 1 min, a CD_2Cl_2 solution (0.4 mL) of $[Rh_2(\mu-Cl)_2(C_2H_4)_4]$ (13.0 mg; 0.0334 mmol). An instant color change was observed, darkening to burgundy within minutes. Free ethylene could be removed (observed by 1H NMR) by freeze-thaw-degassing the solution several times.

Method ii. To a CD_2Cl_2 solution (0.3 mL) of $[Ru(CO)_3(P,P'-dmapm)]$ (**(6)**) (36.5 mg; 0.0493 mmol) was added slowly, over 1 min, a CD_2Cl_2 solution (0.4 mL) of $[Rh_2(\mu-Cl)_2(COD)_2]$ (12.1 mg; 0.0245 mmol). An instant color change was observed, the mixture darkening to a burgundy solution. To remove the liberated COD, the solution was cooled to $-78^\circ C$ and precooled *n*-pentane (20 mL) was added, giving a dark brown/black precipitate, which was found (by $^{31}P\{^1H\}$ NMR spectroscopy) to consist of varying yields (up to a maximum of 80%) of **(7)** together with several unidentified decomposition products. Although this sample was stable for weeks as a solid or in solution at $-78^\circ C$, it decomposed within hours at ambient temperature. MS (EI), using precooled methanol as carrier solvent: m/z 879.0 ($M^+ - H$). Attempts to obtain high-resolution mass spectroscopy data were unsuccessful.

(h) Attempted Reactions of Compounds 1–3 with Metal–Carbonylate Anions. The reaction of compounds **(1)–3** with slight excesses of the metal–carbonylate anions $[PPN][HOs(CO)_4]$ and $Na[FeCp(CO)_2]$ were attempted in a number of solvents (CH_2Cl_2 , THF, acetone, nitromethane) between -80 and $20^\circ C$. After several days either no reaction was observed or small amounts of unidentified species were observed together with mainly starting materials. The $^{31}P\{^1H\}$ NMR spectra of these minor products were inconsistent with the targeted “MM’(μ -dmapm)” geometry, so they were not investigated further. A typical reaction is described as follows: Compound **(1)** (31 mg; 0.043 mmol) was dissolved in 13 mL of THF giving a pale yellow solution, which was subsequently cooled to $-78^\circ C$ in a dry ice/acetone bath. A THF solution (5 mL) of $[PPN][HOs(CO)_4]$ (38 mg; 0.045 mmol) was slowly added via cannula over a 10 min period. The solution was allowed to warm slowly overnight. The solvent was removed in vacuo giving

(19) Wu, Y.-M.; Zou, C.; Wrighton, M. S. *Inorg. Chem.* **1988**, *27*, 3039.

Table 2. Crystallographic Data for Compounds

| | compd 1 | compd 2 | compd 5 | compd 6 |
|--|--|--|--|---|
| formula | C ₃₄ H ₄₂ ClN ₄ OP ₂ Rh | C ₃₄ H ₄₂ ClIrN ₄ OP ₂ | C ₃₅ H ₄₂ Cl ₂ Ir ₂ N ₄ O ₂ P ₂ | C ₃₆ H ₄₂ N ₄ O ₃ P ₂ Ru |
| fw | 723.02 | 812.31 | 1067.97 | 741.75 |
| cryst dimensions (mm) | 0.55 × 0.49 × 0.33 | 0.53 × 0.42 × 0.36 | 0.35 × 0.28 × 0.25 | 0.29 × 0.26 × 0.18 |
| cryst syst | monoclinic | monoclinic | orthorhombic | monoclinic |
| space group | P2 ₁ /c (No. 14) | P2 ₁ /c (No. 14) | P2 ₁ 2 ₁ 2 ₁ (No. 19) | P2 ₁ /c (No. 14) |
| unit cell params | | | | |
| <i>a</i> (Å) | 15.667(2) ^a | 15.7236 (6) ^b | 17.3516(6) ^c | 12.2902(7) ^d |
| <i>b</i> (Å) | 14.431(2) | 14.3785(5) | 20.0932(7) | 16.4522(9) |
| <i>c</i> (Å) | 15.658(2) | 15.6551(6) | 20.9362(7) | 19.015(1) |
| β (deg) | 104.966(2) | 105.026(1) | 90 | 107.735(1) |
| <i>V</i> (Å ³) | 3420.1(6) | 3418.3(2) | 7299.4(4) | 3662.2(4) |
| <i>Z</i> | 4 | 4 | 8 | 4 |
| ρ _{calcd} (g cm ⁻³) | 1.404 | 1.578 | 1.944 | 1.345 |
| μ (mm ⁻¹) | 0.704 | 4.110 | 7.557 | 0.554 |
| diffractometer | Bruker PLATFORM/SMART 1000 CCD | | | |
| radiation (λ [Å]) | graphite-monochromated Mo Kα (0.710 73) | | | |
| temp (°C) | −80 | −80 | −80 | −80 |
| scan type | ω scans (0.3°, 20 s) | ω scans (0.3°, 20 s) | ω scans (0.2°, 20 s) | ω scans (0.3°, 20 s) |
| data collection 2θ limit (deg) | 52.78 | 52.78 | 52.76 | 52.76 |
| total data collected | 25 535 (−19 ≤ <i>h</i> ≤ 19, −18 ≤ <i>k</i> ≤ 18, −19 ≤ <i>l</i> ≤ 19) | 25 961 (−19 ≤ <i>h</i> ≤ 19, −17 ≤ <i>k</i> ≤ 17, −19 ≤ <i>l</i> ≤ 19) | 50 608 (−21 ≤ <i>h</i> ≤ 19, −25 ≤ <i>k</i> ≤ 25, −26 ≤ <i>l</i> ≤ 26) | 27 899 (−15 ≤ <i>h</i> ≤ 15, −20 ≤ <i>k</i> ≤ 20, −23 ≤ <i>l</i> ≤ 23) |
| no. of independent reflns | 6971 (<i>R</i> _{int} = 0.0301) | 6980 (<i>R</i> _{int} = 0.0192) | 14 900 (<i>R</i> _{int} = 0.0297) | 7492 (<i>R</i> _{int} = 0.0330) |
| no. of observed reflns (NO) [<i>F</i> _o ² ≥ 2σ(<i>F</i> _o ²)] | 6182 | 6416 | 14 049 | 6547 |
| abs correction method | multiscan (SADABS) | multiscan (SADABS) | multiscan (SADABS) | multiscan (SADABS) |
| range of transm factors | 0.8010–0.6982 | 0.3192–0.2193 | 0.2538–0.1773 | 0.9068–0.8558 |
| data/restraints/params [<i>F</i> _o ² ≥ −3σ(<i>F</i> _o ²)] | 6971/0/396 | 6980/2 ^e /385 | 14900/0/847 | 7492/0/415 |
| Flack absolute structure param ^f GOF (<i>S</i>) ^g [<i>F</i> _o ² ≥ −3σ(<i>F</i> _o ²)] | 1.110 | 1.037 | −0.001(3) | 1.032 |
| final <i>R</i> indices ^h | | | | |
| <i>R</i> 1 [<i>F</i> _o ² ≥ 2σ(<i>F</i> _o ²)] | 0.0357 | 0.0215 | 0.0210 | 0.0264 |
| <i>wR</i> 2 [<i>F</i> _o ² ≥ −3σ(<i>F</i> _o ²)] | 0.1002 | 0.0560 | 0.0491 | 0.0688 |
| largest difference peak and hole (e Å ⁻³) | 1.456 and −0.490 | 1.647 and −0.635 | 1.522 and −0.342 | 0.444 and −0.283 |

^a Obtained from least-squares refinement of 7288 reflections. ^b Obtained from least-squares refinement of 7781 centered reflections. ^c Obtained from least-squares refinement of 6862 centered reflections. ^d Obtained from least-squares refinement of 8005 centered reflections. ^e The N31A–C32 and N31B–C32 distances were restrained to be 1.44(1) Å. ^f Flack, H. D. *Acta Crystallogr.* **1983**, *A39*, 876–881. Flack, H. D.; Bernardinelli, G. *Acta Crystallogr.* **1999**, *A55*, 908–915. Flack, H. D.; Bernardinelli, G. *J. Appl. Crystallogr.* **2000**, *33*, 1143–1148. The Flack parameter will refine to a value near 0 if the structure is in the correct configuration and will refine to a value near 1 for the inverted configuration. ^g *S* = [Σ*w*(*F*_o² − *F*_c²)/(*n* − *p*)]^{1/2} (*n* = number of data; *p* = number of parameters varied; *w* = [σ²(*F*_o²) + (*a*₀*P*)² + *a*₁*P*]⁻¹ where *P* = [max(*F*_o², 0) + 2*F*_c²]/3). For **1**, *a*₀ = 0.0459, *a*₁ = 3.5716; for **2**, *a*₀ = 0.0278, *a*₁ = 4.3124; for **5**, *a*₀ = 0.0191, *a*₁ = 0; for **6**, *a*₀ = 0.0320, *a*₁ = 1.6202. ^h *R*1 = Σ||*F*_o|| − ||*F*_c||/Σ||*F*_o||; *wR*2 = [Σ*w*(*F*_o² − *F*_c²)/Σ*w*(*F*_o⁴)]^{1/2}.

a yellow residue. Fresh THF (10 mL) was added, and the yellow solution was filtered through Celite. The resulting yellow solution was reduced to ca. 2 mL, and 20 mL of pentane was added, yielding a yellow precipitate. NMR spectra (³¹P{¹H} and ¹H) showed that the major species present were compound **1** and [PPN][OsH(CO)₄] with small amounts (<5% total) of several impurities detected in the ³¹P{¹H} NMR spectrum. The same reaction in acetone yielded only starting material.

X-ray Data Collection and Structure Solution. (a) Yellow crystals of [RhCl(CO)(*P,N*-dmamp)] (**1**) were obtained via slow diffusion of *n*-pentane into a dichloromethane solution of the compound. Data were collected on a Bruker PLATFORM/SMART 1000 CCD diffractometer²⁰ using Mo Kα radiation at −80 °C. Unit cell parameters were obtained from a least-squares refinement of the setting angles of 7288 reflections from the data collection. The space group was determined to be P2₁/c (No. 14). The data were corrected for absorption through use of the SADABS procedure. See Table 2 for a summary of crystal data and X-ray data collection information.

The structure of **1** was solved using the direct-methods program SHELXS-86.²¹ Refinement was completed using the program SHELXL-93.²² Hydrogen atoms were assigned positions based on the geometries of their attached carbon atoms and were given thermal parameters 20% greater than those of the attached carbons.

The final model for **1** was refined to values of *R*1(*F*) = 0.0357 (for 6182 data with *F*_o² ≥ 2σ(*F*_o²)) and *wR*2(*F*²) = 0.1002 (for all 6971 independent data).

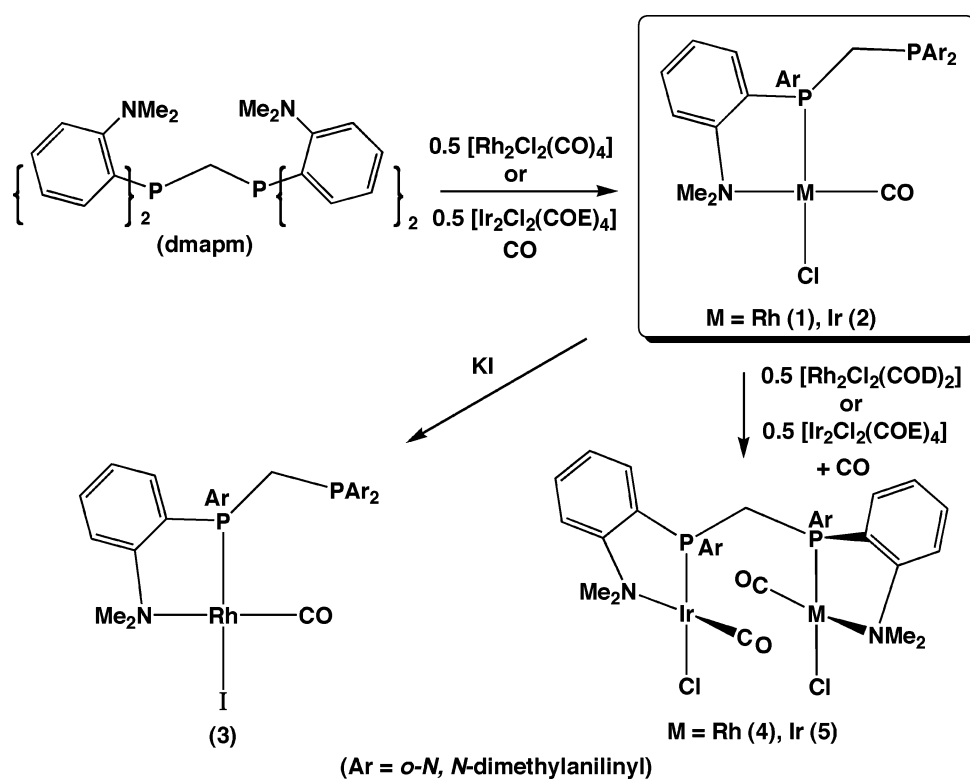
(b) Yellow crystals of [IrCl(CO)(*P,N*-dmamp)] (**2**) were obtained via slow diffusion of *n*-pentane into a dichloromethane solution of the compound. Data were collected and corrected for absorption as for **1** above (see Table 2). Unit cell parameters were obtained from a least-squares refinement of the setting angles of 7781 reflections from the data collection, and the space group was determined to be P2₁/c (No. 14). The structure of **2** was solved, and refinement was completed in the same manner as for **1**, with the same hydrogen atom treatment. One of the dimethylamino groups of **2** was disordered; the major and minor conformers were assigned occupancy factors of 0.55 and 0.45, and the nitrogen-to-ring-carbon distances (N31A–C32 and N31B–C32) were restrained to be 1.44(1) Å. The final model for **2** was refined to values of *R*1(*F*) = 0.0215 (for 6416 data with *F*_o² ≥ 2σ(*F*_o²)) and *wR*2(*F*²) = 0.0560 (for all 6980 independent data).

(20) Programs for diffractometer operation, data collection, data reduction, and absorption correction were those supplied by Bruker.

(21) Sheldrick, G. M. *Acta Crystallogr.* **1990**, *A46*, 467–473.

(22) Sheldrick, G. M. *SHELXL-93: Program for Crystal Structure Determination*; University of Göttingen: Göttingen, Germany, 1993.

Scheme 1



(c) Yellow crystals of $[\text{Ir}_2\text{Cl}_2(\text{CO})_2(\text{P},N,P',N'\text{-dmapm})]$ (**5**) were obtained via slow diffusion of *n*-pentane into a saturated dichloromethane solution of the compound. Data were collected and corrected for absorption as for **1** and **2** above (see Table 2). Unit cell parameters were obtained from a least-squares refinement of the setting angles of 6862 reflections from the data collection, and the space group was determined to be $P2_12_12_1$ (No. 19). The structure of **5** was found to consist of two independent molecules in the unit cell, one having an *S,S* and the other an *R,R* configuration. Solution and refinement proceeded as for compounds **1** and **2**. The final model for **5** was refined to values of $R1(F) = 0.0210$ (for 14 049 data with $F_o^2 \geq 2\sigma(F_o^2)$) and $wR2(F^2) = 0.0491$ (for all 14 900 independent data).

(d) Yellow crystals of $[\text{Ru}(\text{CO})_3(\text{P},P'\text{-dmapm})]$ (**6**) were obtained upon cooling of a solution of the compound in diethyl ether to -80°C . Data were collected and corrected for absorption as for **1**, **2**, and **5** above (see Table 2). Unit cell parameters were obtained from a least-squares refinement of the setting angles of 8005 reflections from the data collection, and the space group was determined to be $P2_1/c$ (No. 14). The structure of **6** was solved using the direct-methods program SIR97;²³ the refinement and hydrogen atom treatment proceeded as for **1**, **2**, and **5**. The final model for **6** was refined to values of $R1(F) = 0.0264$ (for 6547 data with $F_o^2 \geq 2\sigma(F_o^2)$) and $wR2(F^2) = 0.0688$ (for all 7492 independent data).

Results and Compound Characterization

The targeted mononuclear complexes $[\text{MCl}(\text{CO})(\text{P},N\text{-dmapm})]$ ($\text{M} = \text{Rh}$ (**1**), Ir (**2**)) containing the chelating dmapm ligand are readily prepared as outlined in Scheme 1. Although complex **1** can be prepared from the reagents

shown in this scheme at ambient temperature, the yields are variable under these conditions, and the known binuclear complex $[\text{Rh}_2\text{Cl}_2(\text{CO})_2(\mu\text{-P},N,P',N'\text{-dmapm})]$ ²⁴ is invariably present as a contaminant. We have found that carrying out the reaction at -78°C by slow addition of the Rh-carbonyl dimer eliminates this impurity and gives rise to consistently higher yields of the targeted product (**1**).

The $^{31}\text{P}\{^1\text{H}\}$ NMR spectrum of compound **1** displays a doublet of doublets at δ 40.9, having 170 Hz coupling to Rh and 138 Hz coupling to the other phosphorus nucleus, which appears as a doublet at δ -41.8 (see Table 1). Whereas the former resonance is typical of a Rh-bound diphosphine,²⁵ the latter appears near the resonance observed for the free dmapm ligand (δ -36.0).⁷ The $^{13}\text{C}\{^1\text{H}\}$ NMR spectrum displays a single resonance for the carbonyl group at δ 187.8, displaying 73 Hz coupling to Rh and 19 Hz coupling to the adjacent ^{31}P nucleus. The magnitude of this coupling ($^2J_{\text{PC}}$) is typical for a mutually *cis* phosphine and carbonyl arrangement²⁶ and is much smaller than values typical of a *trans* arrangement (ca. 120 Hz).^{26b} In the IR spectrum, the stretch at 1980 cm^{-1} is consistent with a terminal carbonyl involving Rh(I).²⁷ Taken together with the elemental analysis and the mass spectral information, the above spectral data suggest the formulation shown in Scheme 1. Coordination of one of the anilinylyl nitrogens is necessary to give Rh a

(23) Altomare, A.; Burla, M. C.; Camalli, M.; Cascarano, G. L.; Giacovazzo, C.; Guagliardi, A.; Moliterni, A. G. G.; Polidori, G.; Spagna, R. *J. Appl. Crystallogr.* **1999**, *32*, 115–119.

(24) Jones, N. D. Ph.D. Thesis, University of British Columbia, British Columbia, Canada, 2002.

(25) Carlton, L. *Magn. Reson. Chem.* **2004**, *42*, 760.

(26) (a) Mann, B. E. ^{13}C NMR Data for Organometallic Compounds; Mann, B. E., Taylor, B. F., Eds.; Academic Press: London, U.K., 1981; p 23. (b) Rotondo, E.; Battaglia, G.; Giordano, G.; Cusmano, F. P. *J. Organomet. Chem.* **1993**, *450*, 245. (c) Partridge, M. G.; Messerle, B. A.; Field, L. D. *Organometallics* **1995**, *14*, 3527.

(27) Otto, S.; Roodt, A. *Inorg. Chim. Acta* **2004**, *357*, 1.

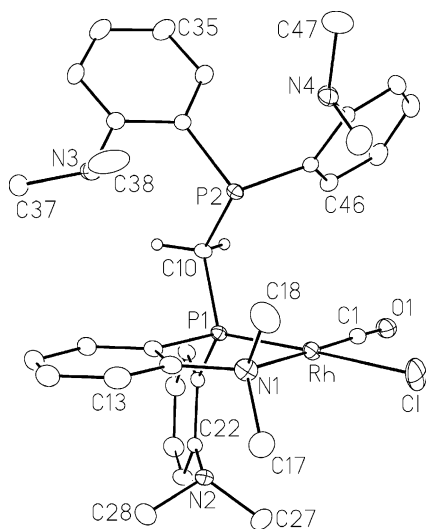


Figure 1. Perspective view of $[\text{RhCl}(\text{CO})(P,N\text{-dmapm})]$ (**1**) showing the atom labeling scheme. Each carbon atom within an anilinyldiphosphine group bears the number of this group (e.g., C(n1)–C(n8)). Non-hydrogen atoms are represented by Gaussian ellipsoids at the 20% probability level. Hydrogen atoms are shown with arbitrarily small thermal parameters for the methylene group of the dmapm ligand; all other hydrogen atoms are omitted.

avored 16-electron, square-planar configuration. At $-80\text{ }^\circ\text{C}$, the ^1H NMR spectrum displays six different methyl resonances for the anilinyldiphosphine methyl groups in a 1:1:2:1:2:1 intensity ratio (see Table 1), consistent with the proposed structure (a detailed interpretation of these data appears later in this section). In contrast to what has been observed for the related species $[\text{PdCl}_2(\text{dmapm})]$, in which isomerism between the P,N -bound and P,P' -bound forms of the ligand was observed, and the Pt analogue $[\text{PtCl}_2(\text{dmapm})]$, which was only observed as the P,P' -bound isomer,⁸ we see no evidence in the NMR spectra for an isomer in which the dmapm is coordinated to Rh through both phosphorus atoms.

The structure proposed for **1** has been confirmed by an X-ray determination, and a representation of the molecule is shown in Figure 1 with selected bond lengths and angles given in Table 3. The chelating dmapm ligand is shown to bind via one phosphorus and an adjacent anilinyldiphosphine group, forming a planar five-membered metallacycle. Completing the square-planar geometry of the metal, the carbonyl ligand lies opposite the anilinyldiphosphine group, with the chloro ligand opposite the coordinated phosphine moiety. In this geometry, the carbonyl and phosphine groups having the greatest trans labilizing effect²⁸ are mutually cis, while the σ -donor amine functionality is opposite the strongest π acceptor. Two pendent groups lie above and below the Rh coordination plane, outside of the immediate coordination sphere. One anilinyldiphosphine group lies below the square plane, having a Rh–N(2) distance of $3.583(2)\text{ \AA}$, while the other end of the diphosphine lies above the plane with a Rh–P(2) distance of $3.5859(7)\text{ \AA}$. Although the Rh–N(2) contact is slightly beyond the van der Waals separation of around 3.40 \AA , the Rh–P(2) distance is within a normal van der Waals contact

of 3.70 \AA .^{22,29} Both contacts are potentially chemically meaningful; the close Rh–N(2) contact has implications in the fluxionality of compound **1**, and the position of P(2) seems ideal for generating a diphosphine-bridged complex by displacement of the chloro ligand by a carbonylate anion, a strategy that we have used successfully in the past for the generation of dppm-bridged heterobinuclear species.³⁰

The structure of **1** is reminiscent of that reported for $\text{PdCl}_2(P,N\text{-dmapm})$,⁸ having a P,N -bound dmapm ligand and also having pendent amine and phosphine moieties on either side of the Pd square-plane, outside of the inner coordination sphere. As was the case for the Pd(II) compound, the structure of **1** allows a comparison to be made of the structural parameters within the coordinated and free phosphine and amine groups. The P–C(aryl) distances ($1.812(3)$, $1.823(2)\text{ \AA}$) and the P–CH₂ distance ($1.832(2)\text{ \AA}$) for the coordinated end of the diphosphine are significantly shorter than those ($1.858(3)$, $1.842(3)$, and $1.865(3)\text{ \AA}$, respectively) of the uncoordinated end. Furthermore, this is accompanied by wider C–P–C angles (range $102.8(1)$ – $105.1(1)^\circ$) for the coordinated end than those (range $97.2(1)$ – $102.9(1)^\circ$) of the free end. Similar trends in the related Pd(II) system have been interpreted,⁸ on the basis of previous arguments,³¹ as indicating that the phosphine is functioning primarily as a σ -donor.

Data for the coordinated amines show an N–C(aryl) bond distance ($1.479(4)\text{ \AA}$) and N–C(methyl) distances ($1.504(4)$, $1.492(4)\text{ \AA}$) that are generally longer than the corresponding distances for the uncoordinated amines (range $1.422(4)$ – $1.438(4)\text{ \AA}$ for the N–C(aryl) and $1.447(4)$ – $1.470(6)\text{ \AA}$ for N–C(methyl)). Also, the angles around the coordinated nitrogens are somewhat more acute (range $108.1(2)$ – $109.5(3)^\circ$) than those of the uncoordinated nitrogens (range $111.0(3)$ – $115.4(3)^\circ$). A similar pattern was noted in $[\text{PdCl}_2(P,N\text{-dmapm})]$.⁸

It is clear from ^1H NMR spectroscopy, presented in Table 1, that there is a high degree of fluxionality within the P,N -chelated complex **1**. At low temperature ($-80\text{ }^\circ\text{C}$), the dimethylanilinyldiphosphine protons exhibit six resonances, assigned to the six different methyl group environments at δ 2.79 (6H_a), 2.26 (6H_b), 3.29 (3H_c), 2.99 (3H_d), 2.65 (3H_e), and 1.54 (3H_f) (see Chart 2 for labeling of the H nuclei). These assignments were established by HMQC, HMBC, spin-saturation-transfer experiments, and ^{31}P -decoupling experiments. According to the solid-state structure shown in Figure 1, there should be four separate resonances for the four inequivalent methyl groups associated with the dangling end of the diphosphine (C(37), C(38), C(47), and C(48)), but even at $-80\text{ }^\circ\text{C}$ only two resonances (H_a and H_b) are observed. Either two pairs

(28) (a) Basolo, F.; Pearson, R. G. *Prog. Inorg. Chem.* **1962**, *4*, 381. (b) Huheey, J. E.; Keiter, E. A.; Keiter, R. L. *Inorganic Chemistry Principles of Structure and Reactivity*, 4th ed.; HarperCollins: New York, 1993; Chapter 13.

(29) (a) Bondi, A. J. *Phys. Chem.* **1964**, *68*, 441. (b) <http://www.webelements.com/webelements/elements/text/H/radii.html>.

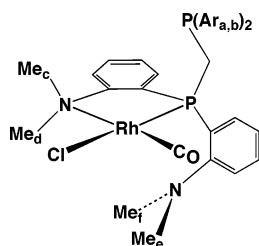
(30) (a) Hiltz, R. W.; Franchuk, R. A.; Cowie, M. *Organometallics* **1991**, *10*, 304. (b) Dell'Anna, M. M.; Trepanier, S. T.; McDonald, R.; Cowie, M. *Organometallics* **2001**, *20*, 88. (c) Antonelli, D. M.; Cowie, M. *Organometallics* **1990**, *9*, 1818. (d) Hiltz, R. W.; Franchuk, R. A.; Cowie, M. *Organometallics* **1991**, *10*, 1297.

(31) (a) Marynick, D. S. *J. Am. Chem. Soc.* **1984**, *106*, 4064. (b) Xiao, S.-X.; Trogler, W. C.; Ellis, D. E.; Berkovitch-Yellin, Z. *J. Am. Chem. Soc.* **1983**, *105*, 7033. (c) Orpen, A. G.; Connelly, N. G. *Organometallics* **1990**, *9*, 1206.

Table 3. Selected Distances and Angles for Compounds **1** and **2**

| | compd 1 (M = Rh) | compd 2 (M = Ir) | | compd 1 | compd 2 | | compd 1 | compd 2 |
|-------------------|---------------------|---------------------|---------------------|-----------|-----------|---------------------|----------|----------|
| Bond Lengths (Å) | | | | | | | | |
| M–Cl | 2.3862(8) | 2.3794(8) | P(2)–C(41) | 1.842(3) | 1.843(3) | N(2)–C(28) | 1.464(4) | 1.460(4) |
| M–P(1) | 2.1921(7) | 2.1934(6) | M–P(2) ^b | 3.5859(7) | 3.5897(7) | N(3)–C(32) | 1.422(4) | <i>a</i> |
| M–N(1) | 2.209(2) | 2.208(2) | O(1)–C(1) | 1.147(3) | 1.154(3) | N(3)–C(37) | 1.470(6) | <i>a</i> |
| M–C(1) | 1.801(3) | 1.804(3) | N(1)–C(12) | 1.479(4) | 1.484(4) | N(3)–C(38) | 1.447(7) | <i>a</i> |
| P(1)–C(10) | 1.832(2) | 1.833(2) | N(1)–C(17) | 1.504(4) | 1.499(4) | N(4)–C(42) | 1.427(4) | 1.425(4) |
| P(1)–C(11) | 1.812(3) | 1.811(3) | N(1)–C(18) | 1.492(4) | 1.499(4) | N(4)–C(47) | 1.460(4) | 1.466(4) |
| P(1)–C(21) | 1.823(2) | 1.828(2) | N(2)–C(22) | 1.438(4) | 1.442(4) | N(4)–C(48) | 1.451(4) | 1.449(5) |
| P(2)–C(10) | 1.865(3) | 1.866(2) | N(2)–C(27) | 1.458(4) | 1.461(4) | M–N(2) ^b | 3.583(2) | 3.628(2) |
| P(2)–C(31) | 1.858(3) | 1.859(3) | | | | | | |
| Bond Angles (deg) | | | | | | | | |
| Cl–M–C(1) | 90.21(9) | 91.67(9) | C(10)–P(2)–C(41) | 102.9(1) | 102.9(1) | C(32)–N(3)–C(37) | 114.3(4) | <i>a</i> |
| Cl–M–N(1) | 92.05(7) | 90.24(7) | C(31)–P(2)–C(41) | 98.1(1) | 97.9(1) | C(32)–N(3)–C(38) | 113.9(3) | <i>a</i> |
| P(1)–M–C(1) | 93.31(9) | 93.68(9) | C(12)–N(1)–C(17) | 108.1(2) | 108.2(2) | C(37)–N(3)–C(38) | 111.9(5) | <i>a</i> |
| P(1)–M–N(1) | 84.42(7) | 84.41(7) | C(12)–N(1)–C(18) | 109.6(3) | 108.6(3) | C(42)–N(4)–C(47) | 115.4(3) | 115.4(3) |
| C(10)–P(1)–C(11) | 102.8(1) | 102.7(1) | C(17)–N(1)–C(18) | 109.5(3) | 109.2(3) | C(42)–N(4)–C(48) | 112.4(2) | 112.7(2) |
| C(10)–P(1)–C(21) | 104.3(1) | 104.2(1) | C(22)–N(2)–C(27) | 112.4(2) | 112.3(2) | C(47)–N(4)–C(48) | 111.0(3) | 111.4(3) |
| C(11)–P(1)–C(21) | 105.1(1) | 104.9(1) | C(22)–N(2)–C(28) | 112.0(2) | 112.1(2) | P(1)–C(10)–P(2) | 108.5(1) | 108.4(1) |
| C(10)–P(2)–C(31) | 97.2(1) | 97.0(1) | C(27)–N(2)–C(28) | 111.3(2) | 111.4(2) | | | |

^a This amine group in compound **2** was disordered over two positions. See the Supporting Information for a complete listing of the parameters. ^b Nonbonded distance.

Chart 2

of resonances are accidentally degenerate or pairs of methyl groups are exchanging at this low temperature. If the latter is the case, it is not clear which pairs are exchanging. At ambient temperature only two resonances are seen at δ 2.71 (12H; H_a and H_b) and 2.60 (12H; H_c, H_d, H_e, and H_f), resulting from rapid exchange of the methyl resonances shown in the respective parentheses. Through a variety of ¹H NMR experiments at various temperatures, we were able to detect three distinct fluxional processes. At -80 °C, ¹H NMR spin-saturation-transfer experiments demonstrate that the anilinyll methyl protons H_c and H_f are exchanging slowly. As the temperature rises, these two resonances broaden until at -40 °C they are almost in the baseline; by -20 °C they have presumably coalesced (although the presence of the other signals makes this difficult to confirm). This process exchanges one set of protons that are in the vicinity of Rh (those on C(27) of Figure 1) with those on C(28) that are aimed away from Rh. We suggest that the protons in the vicinity of Rh are those that resonate at high field (δ 1.54), although the distances of these protons from Rh (the closest Rh–H contact is at 3.24 Å) are beyond the van der Waals separation and appear to rule out an actual agostic interaction involving the methyl group. The exchange of this pair of methyl groups would occur by rotation around the aryl–amine bond (C(22)–N(2)) accompanied by inversion at this nitrogen.³² The second process begins to appear at -40 °C and involves the interconversion of the methyl protons H_a and H_b, as shown by ¹H NMR spin-saturation-transfer

experiments. At 0 °C, H_a and H_b have coalesced to a broad peak that has become sharp by 27 °C. The interconversion of the four methyl groups at these intermediate temperatures must involve a series of inversions at nitrogen and at phosphorus (P(2)) combined with rotation about aryl–amine and the C(1)–P(2) bonds. The third process occurs at approximately 15 °C and involves coalescence of the signals for protons H_c, H_d, H_e, and H_f. This behavior appears to result from exchange of the coordinated and uncoordinated anilinyll groups (associated with N(1) and N(2), respectively) that are bound to the coordinated phosphorus atom. Certainly, the close proximity of N(2) to Rh should facilitate such a process. Again Figure 1 clearly shows how this exchange might be possible. Surprisingly perhaps, no exchange between the bound and unbound phosphorus nuclei is observed in the ³¹P{¹H} NMR spectra, despite the relatively close positioning of P(2) to Rh, shown in Figure 1. We suggest that such an exchange is unfavorable since it would need to involve simultaneous exchange of the coordinated anilinyll group with one of those adjacent to P(2) to maintain the favored five-membered Rh–P–C–C–N metallacycle. In any case, facile exchange of the free and coordinated amine groups, while no exchange of the phosphorus nuclei is observed, is in keeping with the proposed hemilabile nature of the dmampm ligand.

The iridium analogue of compound **1**, namely, [IrCl(CO)-(P,N-dmampm)] (**2**), has been synthesized in a similar manner by the reaction of [IrCl(COE)₂]₂ and dmampm at ambient temperature, under 1 atm of CO. Spectroscopic parameters for this compound are closely comparable with those of **1** (Table 1). The most significant differences (aside from the lack of Rh coupling) appear in the ³¹P{¹H} NMR spectrum in which the chemical shift for the coordinated end of the diphosphine is at significantly higher field (δ 14.2 vs δ 40.9)

(32) Günther, H. In *NMR Spectroscopy: Basic Principles, Concepts, and Applications in Chemistry*, 2nd ed.; Wiley & Sons: New York, 1995; p 357.

than for the Rh analogue, as is commonly observed.³³ Similarly, in the $^{13}\text{C}\{^1\text{H}\}$ NMR spectrum the carbonyl resonance is at higher field and displays coupling to only the *cis*-phosphine. An X-ray structural determination of compound **2** shows that it is almost superimposable on that of **1**, so a representation of this compound is not shown but is given in the Supporting Information. Selected bond lengths and angles are given, together with those of compound **1**, in Table 3 (an identical numbering system was used for both compounds). A comparison of these parameters confirms the close similarity of the two species. Indeed, the same general trends for the phosphine and amine bonding that are seen for **1**—shorter P—C and longer N—C bonds for the coordinated ligands—are also seen for **2**.

Similar fluxional processes to those occurring in **1** are thought to be taking place in **2**, albeit at slightly different temperatures. The exchange process, corresponding to exchange of H_e and H_f protons of **1**, is occurring at $-80\text{ }^\circ\text{C}$ (by ^1H NMR spin-saturation-transfer experiments), with coalescence around $-20\text{ }^\circ\text{C}$. The second process (exchange of H_a and H_b protons) is occurring at $0\text{ }^\circ\text{C}$ in CD_2Cl_2 (as shown by ^1H NMR spin-saturation-transfer experiments). In this case coalescence has not yet been reached by $35\text{ }^\circ\text{C}$ (the temperature limit for CD_2Cl_2). In d^8 -toluene, the resonances for H_a and H_b coalesce around $60\text{ }^\circ\text{C}$. The third process, the exchange of uncoordinated and coordinated anilinylligands, is occurring at $0\text{ }^\circ\text{C}$ in CD_2Cl_2 but again requires higher temperatures in an alternate solvent to reach coalescence ($50\text{ }^\circ\text{C}$ in d^8 -toluene).

Complex **1** reacts with an excess of potassium iodide to yield the iodide analogue, $[\text{Rh}(\text{CO})(P,N\text{-dmamp})]$ (**3**) (Scheme 1). The solvent combination used for this metathesis reaction is a 3:1 methanol–dichloromethane mixture, since no reaction was observed in pure dichloromethane at ambient temperature even after 24 h and an unidentified species was observed using methanol alone. The use of methanol–dichloromethane yielded a pure sample of **3**. All spectral parameters for compound **3** (see Table 1) correspond very closely to those of **1**; the ^{31}P resonance for the pendent phosphine is almost identical in these species as are the ^1H resonances at ambient temperature. Only the ^{31}P resonance for the Rh-coordinated end of the diphosphine differs significantly from that of **1**, appearing at slightly higher field in the iodo species ($\delta\ 37.1$). Furthermore, the carbonyl stretch for the two halide compounds is almost identical at 1980 and 1978 cm^{-1} for **1** and **3**, respectively. All other spectroscopic data, including the fluxional data, are reminiscent of compound **1**.

The binuclear mixed-metal complex $[\text{RhIrCl}_2(\text{CO})_2(P,N,P',N'\text{-dmamp})]$ (**4**) was readily prepared by reaction of $1/2$ equiv of $[\text{RhCl}(\text{COD})]_2$ with $[\text{IrCl}(\text{CO})(P,N\text{-dmamp})]$ (**2**) under an atmosphere of carbon monoxide at ambient tem-

perature and could also be obtained by the reverse reaction of compound **1** with $1/2$ equiv of $[\text{IrCl}(\text{COE})_2]_2$ under carbon monoxide. In the $^{31}\text{P}\{^1\text{H}\}$ spectrum at ambient temperature compound **4** displays a sharp doublet of doublets, corresponding to the Rh-bound end of the diphosphine, at $\delta\ 41.6$ having 176 Hz coupling to Rh and 37 Hz coupling to the other phosphorus nucleus, and it also displays a broad doublet at $\delta\ 13.9$, corresponding to the Ir-bound phosphorus nucleus. Both chemical shifts are in good agreement with the respective values for the coordinated ends of the diphosphines in the Rh and Ir compounds **1** and **2**. Upon the sample being cooled to $-40\text{ }^\circ\text{C}$, the broad high-field signal sharpens to a line-width comparable to that of the Rh-bound end, suggesting a fluxional process occurring at Ir. We have not investigated this further. Selective homonuclear ^{31}P -decoupling experiments confirm the mutual coupling between both ends of the diphosphine. Two resonances are observed in the $^{13}\text{C}\{^1\text{H}\}$ NMR spectrum of a ^{13}CO -enriched sample, corresponding to a Rh-bound ($\delta\ 187.8$; $J_{\text{RhC}} = 75\text{ Hz}$) and an Ir-bound carbonyl ($\delta\ 171.0$). The two expected carbonyl stretches are not resolved in CH_2Cl_2 but can be resolved into a band at 1989 cm^{-1} and a shoulder at 1995 cm^{-1} in acetone.

The diiridium analogue, $[\text{Ir}_2\text{Cl}_2(\text{CO})_2(P,N,P',N'\text{-dmamp})]$ (**5**), is readily obtained upon reacting an equimolar mixture of $[\text{IrCl}(\text{COE})_2]_2$ and *dmamp*, under an atmosphere of CO, and could also be obtained quantitatively in an NMR-scale reaction by combining the mononuclear $[\text{IrCl}(\text{CO})(P,N\text{-dmamp})]$ (**2**) with $1/2$ equiv of $[\text{IrCl}(\text{COE})_2]_2$ under 1 atm of carbon monoxide. Spectral parameters for **5** show some significant differences compared to those of the mononuclear species **2**. In particular, only one resonance is seen in the $^{31}\text{P}\{^1\text{H}\}$ NMR spectrum at a chemical shift ($\delta\ 13.9$) in the region expected for coordination of the phosphine moiety to Ir (see compounds **2** and **4**); this spectrum is also invariant between ambient temperature and $-80\text{ }^\circ\text{C}$. The absence of a resonance corresponding to an uncoordinated end of the diphosphine supports a structure in which two iridium centers are bridged by the diphosphine moiety. Although the $^{13}\text{C}\{^1\text{H}\}$ NMR spectrum shows only one carbonyl resonance, consistent with a terminal carbonyl, the IR spectrum shows two stretches at 1988 and 1979 cm^{-1} . Mass spectral data and elemental analyses support a binuclear formulation in which the two Ir centers are bridged by a single *dmamp* ligand, as shown in Scheme 1. This has been confirmed by an X-ray structure determination, a representation of which is shown in Figure 2, with selected bond lengths and angles in Table 4. The structure shown for **5** is similar to that proposed earlier for the heterobinuclear species $[\text{PtPdCl}_4(\mu\text{-dmamp})]$.^{1a} Several structures are possible for a binuclear species, and the unit cell of **5** contains two independent molecules consisting of a racemic mixture of both *S,S* and *R,R* enantiomers; these are labeled molecule 1 and molecule 2, respectively, in Table 4, which gives selected bond lengths and angles. A representation of molecule 1 is shown in Figure 2. These molecules have the targeted geometry in which the metals are bridged by the diphosphine moiety while each is simultaneously chelated in a *cis* arrangement by an anilinylligand.

(33) (a) Alvey, L. J.; Meier, R.; Soós, T.; Bernatis, P.; Gladysz, J. A. *Eur. J. Inorg. Chem.* **2000**, 1975. (b) Bushweller, C. H.; Rithner, C. D.; Butcher, D. J. *Inorg. Chem.* **1984**, *23*, 1967. (c) Hilts, R. W.; Oke, O.; Ferguson, M. J.; McDonald, R.; Cowie, M. *Organometallics* **2005**, *24*, 4393. (d) George, D. S. A.; Hilts, R. W.; McDonald, R.; Cowie, M. *Organometallics* **1999**, *18*, 5330. (e) Oke, O.; McDonald, R.; Cowie, M. *Organometallics* **1999**, *18*, 1629.

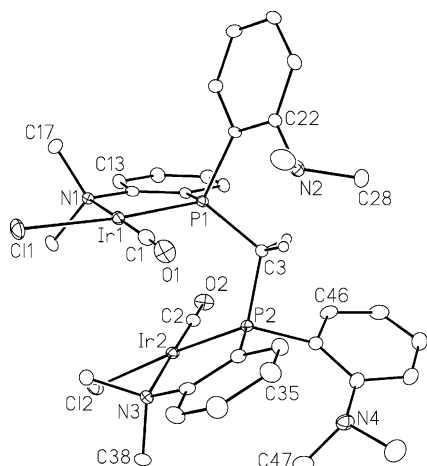
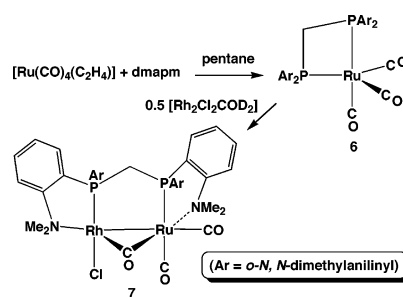


Figure 2. Perspective view of one of the two crystallographically-independent molecules of $[\text{Ir}_2\text{Cl}_2(\text{CO})_2(\text{P},\text{N},\text{P}',\text{N}'\text{-dmamp})]$ (**5**) (molecule 1) showing the atom labeling scheme. Non-hydrogen atoms are represented by Gaussian ellipsoids at the 20% probability level. Hydrogen atoms are shown with arbitrarily small thermal parameters for the methylene group of the dmamp ligand; all other hydrogen atoms are omitted.

group at each end of the molecule. These anilinyllike groups are bound on opposite faces of the Ir_2P_2 plane. Coordination of only one anilinyllike group at each metal renders the phosphorus atoms chiral, and the transoid arrangement of the bound anilinyllike groups, binding to opposite faces of the complex, gives rise to the two observed enantiomers. As in the mononuclear species, **1** and **2**, the phosphines are opposite the chloro ligands while the carbonyls are opposite the amine groups. In fact, a glance at Figures 1 and 2 shows how **5** can result from **2** by coordination of an “ $\text{IrCl}(\text{CO})$ ” group at the pendent phosphine in **2** with concomitant coordination of an anilinyllike group. The two square-planar Ir centers are tilted away from each other by angles of $27.57(4)^\circ$ (molecule 1) and $26.6(2)^\circ$ (molecule 2), and this is clearly demonstrated by the much larger Ir(1)–Ir(2) separation ($4.1272(3)$, $4.3313(3)$ Å) than the P(1)–P(2) separation ($3.156(2)$, $3.217(2)$ Å). This opening up of the diphosphine bite is also seen in the wide P(1)–C(3)–P(2) angles of $118.9(2)^\circ$ and $121.9(3)^\circ$ for the two independent molecules; this angle is 10° wider than those in compounds **1** and **2** in which there are no constraints on the diphosphine bite. In addition to the tilt apart of the square planes, they are staggered with regards to each other by approximately $42\text{--}47^\circ$, with the carbonyl ligand on each metal lying directly above the aryl group of the coordinated anilinyllike group on the other metal. Furthermore, the diphosphine moiety is twisted resulting in an Ir(1)–P(1)–P(2)–

Scheme 2



Ir(2) torsion angle of $41.78(5)^\circ$ and $46.84(4)^\circ$ for the two independent molecules; the effect of this twist is to thrust Ir(1) out of the plane of Figure 2 while Ir(2) lies behind this plane. All twists appear to result from the close contacts between one methyl group on each coordinated anilinyllike group and the chloro ligand on the adjacent metal; these contacts between Cl and the methyl hydrogens (2.9 Å) correspond to van der Waals contacts.

At ambient temperature the ^1H NMR spectrum of **5** shows only four equal-intensity resonances for the anilinyllike methyl groups, reflecting a degree of symmetry in solution. In addition, two of these resonances are broad, and on heating coalesce, suggesting the occurrence of a fluxional process. The two broad peaks sharpen as the temperature is lowered, and spin-saturation-transfer experiments show that exchange is occurring at -20 °C. Two of these four resonances presumably correspond to the coordinated anilinyllike groups, and we suggest that the fluxional process that exchanges the other two occurs by lone pair inversion at the uncoordinated anilinyllike groups. We see no evidence of exchange between the free and coordinated anilinyllike groups indicating that their lability is less than in the mononuclear precursor (**2**).

In attempts to generate potential precursors for mixed-metal group 8/group 9 complexes bridged by dmamp, we chose to investigate mononuclear dmamp complexes of Ru. Reaction of $[\text{Ru}(\text{CO})_4(\eta^2\text{-C}_2\text{H}_4)]$ with dmamp yielded the targeted species $[\text{Ru}(\text{CO})_3(\text{P},\text{P}'\text{-dmamp})]$ (**6**) in good yield, as outlined in Scheme 2. As observed for the diiridium complex (**5**), the $^{31}\text{P}\{^1\text{H}\}$ NMR spectrum of **6** displays only one ligand resonance at $\delta -21.0$, suggesting either a fluxional process that exchanges coordinated and uncoordinated phosphine moieties or a structure in which both phosphorus atoms are coordinated. The invariance of this spectrum over a wide temperature range (down to -80 °C) suggests the latter. Certainly, the relatively high-field chemical shift for this ^{31}P

Table 4. Selected Distances and Angles for Compound **5**

| | molecule 1 | molecule 2 | molecule 1 | molecule 2 | molecule 1 | molecule 2 | | |
|-------------------|------------------------|------------------------|------------------|------------|------------|------------------|-----------------------|-----------------------|
| Bond Lengths (Å) | | | | | | | | |
| Ir(1)–Ir(2) | 4.1272(3) ^a | 4.3313(3) ^a | Ir(1)–C(1) | 1.814(5) | 1.813(5) | Ir(2)–N(3) | 2.192(4) | 2.210(4) |
| Ir(1)–Cl(1) | 2.388(1) | 2.397(1) | Ir(2)–Cl(2) | 2.384(1) | 2.400(1) | Ir(2)–C(2) | 1.818(5) | 1.828(5) |
| Ir(1)–P(1) | 2.187(1) | 2.186(1) | Ir(2)–P(2) | 2.191(1) | 2.192(1) | P(1)–P(2) | 3.156(2) ^a | 3.217(2) ^a |
| Ir(1)–N(1) | 2.192(4) | 2.209(4) | | | | | | |
| Bond Angles (deg) | | | | | | | | |
| Cl(1)–Ir(1)–N(1) | 89.6(1) | 90.7(1) | P(1)–Ir(1)–C(1) | 94.5(2) | 90.9(2) | Cl(2)–Ir(2)–C(2) | 91.0(2) | 90.8(2) |
| Cl(1)–Ir(1)–C(1) | 90.6(2) | 93.8(2) | P(1)–C(3)–P(2) | 118.9(2) | 121.9(3) | P(2)–Ir(2)–N(3) | 85.6(1) | 84.7(1) |
| P(1)–Ir(1)–N(1) | 85.3(1) | 84.6(1) | Cl(2)–Ir(2)–N(3) | 89.4(1) | 90.0(1) | P(2)–Ir(2)–C(2) | 93.9(2) | 94.4(2) |

^a Nonbonded distance.

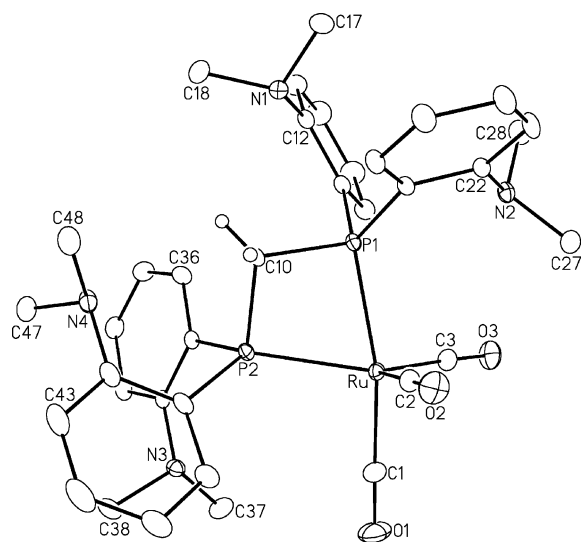


Figure 3. Perspective view of the $[\text{Ru}(\text{CO})_3(\text{P},\text{P}'\text{-dmamp})]$ (**6**) molecule showing the atom labeling scheme. Non-hydrogen atoms are represented by Gaussian ellipsoids at the 20% probability level. Hydrogen atoms are shown with arbitrarily small thermal parameters for the methylene group of the dmamp ligand; all other hydrogen atoms are omitted.

Table 5. Selected Distances and Angles for Compound **6**

| Bond Lengths Å | | | |
|-------------------|-----------|------------------------|-----------|
| Ru–P(1) | 2.3853(5) | Ru–C(2) | 1.909(2) |
| Ru–P(2) | 2.3881(5) | Ru–C(3) | 1.897(2) |
| Ru–C(1) | 1.891(2) | P(1)–P(2) ^a | 2.7651(6) |
| Bond Angles (deg) | | | |
| P(1)–Ru–P(2) | 70.80(2) | P(2)–Ru–C(2) | 102.19(6) |
| P(1)–Ru–C(1) | 168.05(7) | P(2)–Ru–C(3) | 137.69(6) |
| P(1)–Ru–C(2) | 89.21(6) | P(1)–C10–P(2) | 97.40(8) |
| P(1)–Ru–C(3) | 96.76(6) | C(2)–Ru–C(3) | 118.32(9) |
| P(2)–Ru–C(1) | 98.26(7) | | |

^a Nonbonded distance.

resonance is consistent with that of a strained four-membered ring.³⁴ No evidence of a *P,N*-bound diphosphine unit was observed over the temperature range investigated. In the $^{13}\text{C}\{^1\text{H}\}$ NMR spectrum, a single carbonyl resonance (δ 214.3) is observed, which broadens slightly at -80°C , suggesting a fluxional process. The IR spectrum shows three stretches for the terminal carbonyls at 1883, 1910, and 1989 cm^{-1} . The ^1H NMR spectrum of **6** shows only one peak for the aniliny methyl groups at δ 2.12; this resonance broadens on cooling the sample to -80°C , also suggesting the onset of a fluxional process.

An X-ray structural determination of **6** confirms the *P, P'*-binding mode of the diphosphine, in which the phosphorus atoms bind in one axial and one equatorial site of a distorted trigonal bipyramid as shown in Figure 3. Selected bond lengths and angles are given in Table 5. The strain inherent in the four-membered ring formed by the chelating diphosphine is clear, with the P(1)–C(10)–P(2) angle ($97.40(8)^\circ$) being significantly compressed from the idealized value for an sp^3 -hybridized carbon. In addition, the P(1)–Ru–P(2) angle ($70.80(2)^\circ$) is much less than the idealized 90° ,

resulting in a significant deviation of P(1) from the axial site opposite C(1)–O(1), as demonstrated by the P(1)–Ru–C(1) angle of $168.05(7)^\circ$. This strain also results in distortion within the trigonal plane leading to widely different P(2)–Ru–C(2) ($102.19(6)^\circ$), P(2)–Ru–C(3) ($137.69(6)^\circ$), and C(2)–Ru–C(3) ($118.32(9)^\circ$) angles.

Clearly, the X-ray structure indicates that both phosphorus nuclei are inequivalent, one (P(1)) occupying an axial site and one (P(2)) occupying an equatorial site. The observation of only one resonance in the $^{31}\text{P}\{^1\text{H}\}$ NMR spectrum (even down to -80°C) suggests that these nuclei are exchanging rapidly, presumably by a Berry pseudorotation process.³⁵ Similar fluxionality was reported in a series of $\text{Ru}(\text{CO})_3\text{L}_2$ complexes, in which L_2 represents chelating diphosphines.³⁶ This proposed fluxionality also explains the appearance of only a single carbonyl resonance in the $^{13}\text{C}\{^1\text{H}\}$ NMR spectrum.

Compound **6** reacts with $1/2$ equiv of either $[\text{Rh}_2(\mu\text{-Cl})_2(\text{COD})_2]$ or $[\text{Rh}_2(\mu\text{-Cl})_2(\text{C}_2\text{H}_4)_4]$ to give the same mixed rhodium/ruthenium-containing product $[\text{RhRuCl}(\text{CO})_2(\mu\text{-CO})(\text{dmamp})]$ (**7**) in each case (by $^{31}\text{P}\{^1\text{H}\}$, ^1H NMR, and IR spectroscopy), as outlined in Scheme 2. With $[\text{Rh}_2(\mu\text{-Cl})_2(\text{CO})_4]$, the same product, in 31% yield, is seen by $^{31}\text{P}\{^1\text{H}\}$ NMR spectroscopy but with a number of additional unidentified species. In the $^{31}\text{P}\{^1\text{H}\}$ NMR spectrum, at ambient temperature, this new compound shows two mutually coupled resonances at δ 50.5 (dd, $^2J_{\text{PP}} = 107$ Hz, $^1J_{\text{RhP}} = 179$ Hz) and δ 34.2 (d, $^2J_{\text{PP}} = 107$ Hz). The low-field chemical shift of both resonances, which differ substantially from that observed for the free ligand ($\delta = -36.0$), as well as the Rh-coupling observed in the former, indicates that the dmamp ligand bridges rhodium and ruthenium centers through its two phosphorus atoms. The $^{13}\text{C}\{^1\text{H}\}$ NMR spectrum confirms the presence of three carbonyl ligands, two of which are terminally bound to ruthenium at δ 203.1 and 197.3, while the third, at δ 246.3, is bridging. The former Ru-bound carbonyl displays a large coupling (102 Hz) to phosphorus that is typical for a trans arrangement of carbonyl and phosphine groups,^{21b} while the bridging carbonyl shows 42 Hz coupling to Rh and additional coupling to both ^{31}P nuclei. Additional support for the formulation shown in Scheme 2 comes from the IR spectrum of **7**, which shows two terminal carbonyl stretches at 2001 (s) and 1908 (m) and a bridging stretch at 1726 (w) cm^{-1} . Our attempts to isolate complex **7** for elemental analysis and X-ray crystallography have been unsuccessful; although reaction solutions of this species are stable at ambient temperature for short periods of time, any attempt to isolate a pure species by recrystallization resulted in its decomposition. Solutions of **7**, prepared using $[\text{Rh}_2(\mu\text{-Cl})_2(\text{C}_2\text{H}_4)_4]$, were slightly more stable (up to 1 day at ambient temperature), even upon removal of the ethylene by freeze–thaw–degassing the solution several times. However, again attempts to isolate

(34) See the following for examples: (a) Bickley, J. F.; La Pensée, A. A.; Higgins, S. J.; Stuart, C. A. *J. Chem. Soc., Dalton Trans.* **2003**, 4663. (b) Higgins, S. J.; La Pensée, A. A.; Stuart, C. A.; Charnock, J. M. *J. Chem. Soc., Dalton Trans.* **2001**, 902. (c) Garrou, P. E. *Chem. Rev.* **1981**, 81, 229.

(35) (a) Shriver, D. F.; Atkins, P. W. In *Inorganic Chemistry*, 3rd ed.; W. H. Freeman and Co.: New York, 1999; Chapter 7. (b) Berry, R. S. *J. Chem. Phys.* **1960**, 32, 933.

(36) Buntin, K. A.; Farrar, D. H.; Poë, A. J.; Lough, A. J. *Organometallics* **2000**, 19, 3674.

the solid led to decomposition. Our inability to isolate compound **7** from solution initially suggested a possible involvement of residual coordinated olefin, but this seems unlikely on the basis that the spectroscopic parameters for products prepared from COD, COE, and ethylene-containing precursors were superimposable. In addition, the above solutions could be obtained essentially free of the olefin by degassing the solutions and could also be obtained in the complete absence of olefins in the reaction of **6** with $[\text{Rh}_2\text{Cl}_2(\text{CO})_4]$. Solvent also appeared not to influence stability, with similar behavior obtained in a number of solvents.

The structure proposed for **7** is reminiscent of a series of dpmm-bridged complexes $[\text{Rh}_2\text{X}_2(\mu\text{-L})(\text{dpmm})_2]$ ($\text{X} = \text{Cl}, \text{Br}$; $\text{L} = \text{CO}, \text{SO}_2, \text{CF}_3\text{C}_2\text{CF}_3$),^{37–39} except in having an extra ligand bound to Ru, giving this metal its favored 18e configuration. In particular, compound **7** has a low-frequency stretch for the bridging carbonyl that is reminiscent of those in the dpmm-bridged species, $[\text{Rh}_2\text{X}_2(\mu\text{-CO})(\text{dpmm})_2]$.³⁷

Discussion

In previous studies we have reported a convenient route to binuclear mixed-metal complexes of groups 8 and 9 metals through chloride displacement from the group 9 complexes $[\text{MCl}(\text{dpmm})_2]$ ($\text{M} = \text{Rh}, \text{Ir}$) by the metal–carbonylate anions $[\text{M}'\text{H}(\text{CO})_4]^-$ ($\text{M}' = \text{Ru}, \text{Os}$), yielding the products $[\text{MM}'\text{H}(\text{CO})_3(\text{dpmm})_2]$.³⁰ As noted in the Introduction, we sought to extend this chemistry to the dmapm ligand, in which the diphosphine moiety could bridge the metals while a pair of anilinyll groups could chelate, one to each metal, via the amine nitrogens. Such a binding mode would give a cis arrangement of this multidentate ligand at each metal, in contrast to the usual trans arrangement of the disphosphines in the dpmm-bridged complexes noted above (Chart 1). A pair of obvious mononuclear precursors for employing such a strategy are the complexes $[\text{MCl}(\text{CO})(P,N\text{-dmapm})]$ ($\text{M} = \text{Rh}$ (**1**), Ir (**2**)). These species were readily prepared as outlined earlier in Scheme 1 and have the expected square-planar geometry, in which the dmapm ligand is bound to the metal via one phosphorus and one of the adjacent anilinyll nitrogens. The resulting five-membered M-P-C-C-N metallacycle is relatively unstrained and is certainly much less so than the four-membered M-P-C-P metallacycle that would result had the ligand been bound to the metal via both phosphorus atoms. The structures of both the rhodium and the iridium species suggested that these complexes would be promising precursors for the synthesis of heterobinuclear species, owing to the positioning of the pendent phosphine, immediately above the metal, seemingly in an ideal position to coordinate a second metal.

The suitability of dmapm as a bridging group in group 9 metal chemistry is clearly demonstrated in the rhodium–iridium (**4**) and diiridium species (**5**), as shown for the latter in Figure 2. The geometry adopted for the diiridium product

has the chelating amine groups on opposite faces of the Ir_2P_2 plane as shown earlier for structure **B**, rather than on the same face, as diagrammed in structure **C**. The observed arrangement of the dmapm substituents is adopted in order to minimize contacts between the methyl groups on the coordinated amines, which would be very unfavorable in structure **C**. A similar geometry was proposed involving the group 10 metals Pd and Pt.^{1a}

Our strategy of generating mixed-metal complexes, bridged by the dmapm ligand, through chloride displacement from $[\text{MCl}(\text{CO})(P,N\text{-dmapm})]$ by the carbonylate anion, $[\text{OsH}(\text{CO})_4]^-$, did not succeed. Similarly, use of a strong nucleophile such as $\text{Na}[\text{FeCp}(\text{CO})_2]$ ⁴⁰ also gave no reaction as did attempts to displace the iodide ion from $[\text{Rh}(\text{CO})(P,N\text{-dmapm})]$ (**3**) by these anions. Certainly, the successful replacement of the chloride anion in **1** by the iodide ion to give **3** indicates that nucleophilic displacement by small anions is possible.

One problem with our anion-displacement strategy for the generation of dmapm-bridged heterobinuclear complexes appears to be the geometry of the precursor (**1**), in which the halide lies opposite the Rh–phosphorus bond. To maintain the favored square-planar geometry at Rh, the metal–carbonylate anion must bind opposite the Rh–P bond at the site of the displaced halide (see Figure 1). In this site the added metal is too far from the pendent phosphorus to allow coordination of the latter. Although one can envision a rearrangement at Rh that would bring the added metal to a site cis to the Rh-bound end of the diphosphine in a position appropriate for binding of the pendent end, this would place two ligands (CO, phosphine) having a high trans effect opposite each other, destabilizing this arrangement. Furthermore, as discussed for compound **5** and as shown in Figure 2, destabilizing interactions involving the methyl groups on the coordinated amine and ligands on the adjacent metal cannot be overlooked. In the previously structurally characterized compounds in which a dmapm group bridges a metal–metal bond,^{1a,8} both group 10 metals have a relatively uncrowded square-planar geometry in which the remaining three sites, besides the metal–metal bond, are occupied by dmapm (*P*- and *N*-bound) and a chloro ligand. The incorporation of the group 8 metals, Ru and Os, into dmapm-bridged complexes will give rise to additional nonbonding repulsions between ligands and the dmapm substituents owing to the tendencies of these earlier metals to be coordinatively saturated and to consequently have higher coordination numbers.

An alternate strategy for generating a heterobinuclear complex of Rh and Ru is to start with a diphosphine complex of the latter and to react it with an appropriate Rh species. The targeted complex $[\text{Ru}(\text{CO})_3(P,P'\text{-dmapm})]$ (**6**) was synthesized by ethylene displacement from $[\text{Ru}(\text{C}_2\text{H}_4)(\text{CO})_4]$. Unlike the mononuclear analogues of the group 9 metals (**1–3**), in which the dmapm ligands are bound through one phosphine and one amine functionality, the Ru species is coordinated to dmapm through both phosphorus atoms. The

(37) (a) Cowie, M.; Dwight, S. K. *Inorg. Chem.* **1980**, *19*, 2508. (b) Gelmini, L.; Loeb, S. J.; Stephan, D. W. *Inorg. Chim. Acta* **1985**, *98*, L3.

(38) Cowie, M.; Dwight, S. K. *Inorg. Chem.* **1980**, *19*, 209.

(39) Cowie, M.; Dickson, R. S. *Inorg. Chem.* **1981**, *20*, 2682.

(40) King, R. B. *Acc. Chem. Res.* **1970**, *3*, 417.

P,P'-binding mode is initially surprising, generating a highly strained, four-membered Ru–P–C–P metallacycle instead of a more favorable five-membered Ru–P–C–C–N metallacycle as observed in compounds **1** and **2**. However, the preference of the “Ru(CO)₃” unit for the softer phosphine than the harder amine group⁴¹ presumably overcomes the unfavorable ring strain. In the case of compounds **1** and **2**, the “MCl(CO)” unit is slightly harder (M(+1) vs Ru(0)), so its preference for the softer phosphine linkage is less, allowing ring strain to dominate. In any case, the highly strained Ru–P–C–P ring fits our strategy for generating heterobinuclear complexes, a strategy that has previously been exploited,^{30,42} in which the strained diphosphine readily unwinds to adopt a relatively unstrained bridging arrangement. In this case, the reaction of **6** with an appropriate source of “RhCl” generates the dmamp-bridged product [RhRuCl(CO)₂(μ-CO)(*P,N,P',N'*-dmamp)] (**7**), as shown in Scheme 2. Unfortunately, this product is unstable, decomposing upon workup, so a full structural analysis was not possible. As noted earlier, steric crowding involving the *o*-*N,N*-dimethylaniliny groups on one metal and ligands on the adjacent metal will tend to destabilize a metal–metal bonded species. This destabilization will clearly become more problematic with earlier metals than Rh, owing to their higher coordination numbers. In compound **7**, the metal–metal bonded species seems possible owing to the geometry at Rh, in which we propose that the coordinated amine is opposite the Rh–Ru bond as observed for the terminally bound groups in related carbonyl-bridged dpmm compounds.³⁷ Such an arrangement allows the coordinated dimethylaniliny groups to avoid each other. Nevertheless, the steric crowding that results from the higher coordination number at Ru may contribute to the instability of this compound.

Conclusions

The dmamp ligand displays a versatile coordination chemistry in which it can chelate to a single metal, binding

either through adjacent phosphine and amine functionalities or by both phosphine groups. Although the former binding mode is favored by less strain within the resulting five-membered metallacycle, the latter can be formed by soft metal centers despite the resulting strained four-membered metallacycle. This ligand can also bridge metals through the diphosphine moiety in which a neighboring amino group on each end of the diphosphine can also chelate to the adjacent metal. Although we did not succeed in synthesizing the targeted group 8/group 9 metal complexes by the anticipated route, we did succeed in generating a diridium species, a mixed Rh/Ir analogue, and a Rh/Ru species by alternate routes. The potential of dmamp to function as a bridging ligand that is capable of enhancing metal–metal cooperativity in heterobinuclear complexes of group 8 and group 9 metals and the roles of the coordinated amines as labile groups for the generation of coordinative unsaturated species remain to be demonstrated. These topics will form the basis of subsequent investigations.

Acknowledgment. We thank the Natural Sciences and Engineering Research Council of Canada (NSERC) and the University of Alberta for financial support of this research and NSERC for funding the Bruker PLATFORM/SMART 1000 CCD diffractometer and the Nicolet Avator IR spectrometer. We also thank Dr. N. D. Jones for helpful discussions.

Supporting Information Available: X-ray experimental details, atomic coordinates, interatomic distances and angles, anisotropic thermal parameters, hydrogen parameters for compounds **1**, **2**, **5** and **6** in a CIF file and a perspective view (ORTEP) of compound **2**. This material is available free of charge via the Internet at <http://pubs.acs.org>.

IC051639C

(41) (a) Pearson, R. G. *J. Am. Chem. Soc.* **1963**, *85*, 3533. (b) Huheey, J. E.; Keiter, E. A.; Keiter, R. L. *Inorganic Chemistry Principles of Structure and Reactivity*, 4th ed.; HarperCollins: New York, 1993; Chapter 9.

(42) See the following for examples: (a) Hutton, A. T.; Pringle, P. G.; Shaw, B. L. *Organometallics* **1983**, *2*, 1889. (b) Iggo, J. A.; Markham, D. P.; Shaw, B. L.; Thornton-Pett, M. *J. Chem. Soc., Chem. Commun.* **1985**, 432. (c) Blagg, A.; Shaw, B. L. *J. Chem. Soc., Dalton Trans.* **1987**, 221. (d) Blagg, A.; Pringle, P. G.; Shaw, B. L. *J. Chem. Soc., Dalton Trans.* **1987**, 1495.